Regional character of geomagnetic field directional circularity: Holocene Eastern North America

Steven P. Lund
Dept. Earth Sciences, University of Southern California

Abstract

This study summarizes paleomagnetic secular variation (PSV) in five published Holocene records from Eastern North America. We have developed 100-year increment time series for the declinations and inclinations for all sites and compared their directional variability. We see evidence of ten correlatable features in both inclination and declination. We focus on the clockwise or counter-clockwise motion of paleomagnetic directions (termed circularity) in these PSV records. We have first calculated the incremental rate and direction of motion (clockwise or counter-clockwise) for each record over the last 4000-8000 years. We have separately looked for discernable looping in individual records. We estimate the loop sizes, durations, and circularity direction. We see the same pattern of circularity in both measurement techniques. There are seven intervals of oscillating circularity and looping in all five sites. Both techniques suggest a distinctive oscillating, teeter-totter like, behavior to PSV circularity that must be due to the pattern of fluid flow in the outer core. This teeter-totter behavior is unbalanced with more time spent in clockwise motion than in counter-clockwise motion. We think the teeter-totter oscillation may be due to torsional oscillation in the outer core fluid flow. The loops have a distribution of sizes and durations with smaller loops being shorter in duration and bigger loops having longer durations. All five PSV records show 5 intervals of ~10^2 yr significant acceleration in circularity rate and PSV rate combined with change in circularity direction. These features are broadly analogous to historic geomagnetic jerks.

Introduction

The geomagnetic field that we measure (poloidal field) is largely generated in the Earth's liquid outer core by dynamo activity (flux regeneration). (See Merrill et al. (1998) for overview.) One goal in studying the geomagnetic field is to understand the space/time pattern of geomagnetic field variability (secular variation) and infer from that the pattern of fluid dynamo activity in the outer core that maintains/regenerates the field. Flux regeneration is associated with the turbulent flow of liquid iron in the outer core that twists magnetic field lines and generates new flux in the process.

Historical secular variation (HSV) of the geomagnetic field measured at a single location was first identified by Gellibrand in 1634 (Merrill et al., 1998). Halley in 1692 (Merrill, et al., 1998) noted that mapped geomagnetic field directions tended to drift westward over time. Runcorn (1959) associated secular variation with movements of magnetic sources in the Earth's outer core and suggested that clockwise (counter-clockwise) motion of directions at a single locality over time (herein termed circularity) could be due to westward (eastward) motion of the magnetic sources in the outer core. Skiles (1970) developed this idea further and noted some degree of ambiguity in relating clockwise versus counter-clockwise motion of directions with westward versus eastward drift. There is now very clear evidence for both clockwise and counter-clockwise motion of directions within different regions of the Earth for both HSV (e.g., Thompson and Barraclough, 1982; Gubbins and Bloxham, 1987) and paleomagnetic field secular variation (PSV) (e.g., Lund and Banerjee, 1985; Smith and Creer, 1986; Itota et al., 1997).

This study is the second in a series (Lund, 2020) to evaluate the Holocene (millennial-scale) character of directional PSV (circularity) in a region, in this case Eastern North America (Figure 1), using two different techniques to quantify the directional circularity pattern. The goal is to determine if more specific information about fluid flow in the outer core can be estimated by more carefully assessing the pattern of PSV circularity on a regional scale.

The Character of Circularity

Geomagnetic field directional secular variation at a locality that is high-resolution (good serial correlation of successive data points) can be plotted through time in inclination (I)/declination (D) space (traditionally referred to as a Bauer plot (Bauer, 1895)). Most of the time the directional variability displays open loops, either clockwise or anti-clockwise (e.g., Runcorn, 1959; Kawai et al., 1965). The loop durations run from a few hundred years to more than one thousand years, often with short loops superposed on longer loops (e.g., Lund and Banerjee, 1985). On occasion, I and D track together to create a linear trend (e.g., Doell and Cox, 1965; Turner et al., 1982; Evans, 1984). Loops can occur as a result of large dipole variations; in such a case, the looping pattern should be temporally coherent over much of the Earth (Kawai et al. 1965). However, studies of HSV or longer-term (Holocene) PSV looping tend to indicate that looping varies coherently over limited spatial domains up to ~4000 km; beyond that spatial domain, the looping ordinarily changes style (Thompson and Barraclough, 1982; Bloxham et al., 1989).

Open looping could be due to motion of small field sources near the core/mantle boundary in the outer core located under a locality. Two models of such localized field are radial dipoles (Alldredge and Hurwitz, 1964) or dynamo waves (Olson and Hagee, 1987; Hagee and Olson, 1989). Clockwise looping was generally associated with westward motion of small dipole sources, while counterclockwise looping was associated with eastward motion (Runcorn, 1959; Skiles, 1970). These ideas were non-unique however (Dodson, 1979), and poleward propagation of dynamo waves could produce the same clockwise or counterclockwise looping (Olson and Hagee, 1987; Hagee and Olson, 1989). More recent analyses of millennial-scale PSV suggest a variety of other ways that observed circularity might occur (e.g., Dumberry and Bloxham, 2006; Constable, 2011; Korte et al., 2011; Davies and Constable, 2018).

Models of secular variation that produce open looping are associated with an out-of-phase relationship between I and D. This distinctive directional waveform pattern is common in both HSV and PSV. On occasion, evidence has been noted for more complicated, longer-term directional waveforms (e.g., Lund et al., 1988; Negrini et al., 1994). But, this paper only considers the simplest pattern. The size of the open loops depends on the amplitude of I and D cycles; the duration depends on the time interval of each I/D cycle.

Looping can be considered an indicator of dynamo turbulence directly below the PSV record locality. The fact that the pattern of looping varies over the Earth suggests that dynamo turbulence has a regional character. One question is whether adjacent regions share any degree of correlation. The focus of this paper is to more carefully assess the actual pattern of circularity and its range of complexity as a starting point for later assessing its relationship to potential patterns of dynamo activity.

Regional Pattern of PSV Circularity

There are five sites in Eastern North America that have high-resolution, well-dated PSV records for the last 4,000-8,000 years (Figure 1; Table 1; Appendix 1). The studies come from three lake sediment studies (Sandy Lake PA (SAN), Lake Lebeouf PA (LEB), and Seneca Lake NY (SEN)), and two deep-sea sediment studies (Core 2220 and the East Canada Stack (ECS)). All of these sites have records of both inclination and declination variability. All of them have high-resolution dating that provides a chronostratigraphic framework for their comparison (Table 1). The main goal of this paper is to determine the pattern of PSV variability through time within a region where the PSV records should have strong similarity. Several of these records have been previously analyzed by Lund (1996) and Lund et al. (2021). The key features of the PSV records described below are 1) that they all have age dating with resolution to ~±100 years or so, and 2) that the PSV data have strong serial correlation such that clear correlatable inclination and declination features based on multiple measurements can be discerned and correlated with the other records. Below is a summary of the paleomagnetic data and chronostratigraphy for each site.

Sandy Lake PA (SAN) was studied by King (1983). The lake has a 6000-yr PSV record that was dated by 8 radiocarbon dates. Lake LeBeouf PA (LEB) and Seneca Lake NY (SEN) were studied by King (1983) and King et al. (1983). LEB has a 4000-yr PSV record dated by 6 radiocarbon dates. SEN has an 8000-yr PSV record that is dated by 4 radiocarbon dates. All three of these PSV records were compared with other North American PSV records by Lund (1996). Lund (1996) also provided a correction to the radiocarbon dating so the records use here are in absolute years AD/BC. Core 2220 from the St. Lawrence Estuary was studied by St. Onge et al. (2003). The core was dated by 6 calibrated radiocarbon dates. A stack for eastern Canada Holocene PSV records (ECS) was developed by Barletta et al. (2010). The stack includes core 2220 and five other PSV records from the same St. Lawrence

Estuary region. Barletta et al. (2010) developed a calibrated age model for all these records based on 30 radiocarbon dates.

An estimate of sample error for the sediment records has been determined by calculating the mean and standard deviation (1 sigma) for stratigraphic intervals of 3 successive sample measurements. The hypothesis is that the 1-sigma uncertainty is the maximum estimate of error for that interval by assuming that there is no field difference among the three measurements over such a short time interval. In reality, there will be some small trend in the three successive measurements due to real changes in the paleomagnetic field. So the 1-sigma error incorporates some real error in measurement and some variation in field.

Figures 2 and 3 show the inclination and declination records of the five PSV records for the last 3000 years (small closed circles). The records all have error envelopes of ±1 sigma. We also show the summary of historical measurements (open squares) for the last ~400 years, termed gufm1 (Jackson et al., 2000). We have developed equi-spaced time series in 100-yr increments for all of these PSV studies (larger solid circles connected in Figures 2 and 3). There are 10 reproducible scalar features in the inclination and declination records (a-j in Figures 2, 3). The resultant equi-spaced time series are summarized in Table 1 and listed in Appendix 1. These time series are part of a large group of equi-spaced Holocene PSV time series from around the World termed PSVMOD2.0 (total of 87 sites). The typical directional difference between the actual PSV data and their PSV models is less than ±1°.

We have grouped these five sites together because they are largely closer to one another than any other Holocene PSV sites within PSVMOD2.0. Even so, it is worth considering, as we move forward with the data analysis, whether these five sites all represent the same regional sense of dynamo activity in the outer core below them. The fact that all five sites share most or all of the same simple scalar PSV features (Figures 2, 3), is one measure that they all do covary, in some sense of the word. The fact that the individual scalar features are not exactly synchronous could simply be due to some error in the site chronologies.

Circularity Estimates

We have estimated circularity of the vector time series in two ways. We first calculated the amplitude and direction of circularity in the smallest time interval available to us – 200 years or three successive data points. Figures 4 (a, b) show two examples of 200-yr circularity intervals. Three successive paleomagnetic directions are needed to define any arcuate motion. If the three directions fall on a straight line, then there is no circularity. But, if the three directions form a triangle with some discrete area, as in Figure 4 (a, b), then we can estimate both the direction of circularity, clockwise (C) or counterclockwise (CC), and the 'amplitude' of the circularity defined by the triangular area associated with the three points. We have also calculated the circularity for an interval of five successive points (400 yrs). This gives a more smoothed estimate of circularity, but helps to define intervals among the records with a common sense of circularity. All calculations were done in 100-yr steps or increments with the central year (of three or five data points) defining the calculation year.

The results of the three-point (200 yr) circularity calculation for all five sites over the last 3000 years are shown in Figure 5 (open circles). The value magnitudes indicate the area of the three-point triangles (in arc degrees squared) with positive values indicating clockwise motion and negative values indicating counterclockwise motion. There are occasionally amplitudes that are almost zero, indicating simple linear, not arcuate, motion for each 200-yr increment. But, more than 90% of the values do indicate some sense of circularity. The results of the five-point (400 yr) circularity calculation for all five sites over the last 3000 years are shown in Figure 5 (closed circles). This gives a more smoothed/integrative sense of circularity. All five sites seem to show the same general pattern of circularity with 300-900 years of one sense of circularity alternating with the other sense of circularity. We have labeled seven alternating intervals of circularity (A-G).

There is generally good circularity agreement among the five time series, but the interval from 500-1000 AD is marked by low amplitude circularity and SEN, 2220, and ECS have some evidence of small amplitude counterclockwise circularity while the other two time series have small amplitude clockwise circularity. This is probably an artifact of the data. Overall, all five records show the same 7 alternating counter-clockwise/clockwise pattern of circularity.

The second way to estimate circularity is to look for notable intervals of looping in the time series. We looked primarily for complete loops (usually five or more points (>400 yrs of circularity), but accepted partial loops that appeared to be at least ½ loop (Figure 4c). The difference in this method is that we ignored small intervals of one sense of looping (<< ½ loop) if they fell within a larger pattern of looping of the opposite sense. In this way, we typically identified 7 complete or partial loops in all five time series. That is the same number of looping intervals noted above by the time series analysis. Table 2 summarizes the loops in each time series. Figure 5 shows the intervals of notable looping to the right of each site (black intervals are clockwise loops, white intervals are counterclockwise loops). Transitions between clockwise and counter-clockwise looping studied in this manner allow 100-300 year overlaps in circularity sense. We labeled the notable loops α-ν (numbers in parentheses indicate a whole loop or partial loop) and we see evidence for each of these loops in all five time series. The loops are present in all the PSV sites and almost all the correlatable loops are the same sense of circularity. Some loops are a bit longer or shorter in duration than others from the same time interval and there is some variation in overall size of comparable loops.

Figure 6 plots the pattern of circularity in four intervals. Figures 6 (a, b) plot the circularity at LEB and ECS for the last 1500 years. They clearly show the alternating C/CC oscillations in circularity that are summarized in Figure 5. Figures 6 (c, d) plot the circularity at LEB and SEN for 500 AD-1000 BC. Here, too, one can see a clear alternation of circularity as summarized in Figure 5.

We can estimate the size of each loop by calculating the inclination and declination span for each loop (Table 2). Some loops are quite large and the declination span (but not the inclination span) is affected by site latitude. Therefore, we have normalized the declination spans by COS(site latitude). We have calculated an overall ‘amplitude’ for each loop as the RMS of the inclination and normalized declination spans. The loop ‘amplitudes’ and durations (for a complete loop) are plotted in Figure 7 (top). There appears to be a fairly linear trend with smaller amplitude loops having shorter durations and larger amplitude loops having longer durations. There is also a bias for larger amplitude/longer duration loops being clockwise.

This is almost identical to the circularity pattern for Holocene East Asia (Lund, 2020) shown in Figure 7 (bottom). Here, too, the looping pattern has shorter-duration (longer-duration) loops being smaller (larger) in amplitude and the largest/longest loops being clockwise. Thus, there is here, too, a bias to clockwise circularity over counter-clockwise circularity. Also, in both regions, the circularity pattern is an alternation of clockwise versus counter-clockwise looping with neither lasting much more than one full loop. This teeter-totter effect is very distinctive and also seems to be presents in recent longer-duration Pleistocene PSV records now under analysis (Lund, in review). These are the only two Holocene regions to undergo this type of circularity analysis. Yet, it seems that this distinctive pattern may be normal for overall PSV. Further studies are under way to test these observations further.

Three of the PSV time series (SEN, 2220, ECS)) are 8000 years in duration. We plot these time series in Figure 8. We plot their circularity rates in Figure 9. The horizontal tie lines indicate intervals of clockwise or counterclockwise circularity that the sites have in common. Intervals A-G are also shown in Figure 5. Circularity is more subdued before 1000 BC. This may be a matter of reduced data resolution, but the same pattern is noted in the East Asia data (Lund, 2020).

One last observation with respect to Eastern North America PSV circularity is that most or all five sites share the same short-duration, but largest-rate, circularity intervals. The Circularity rates of all five sites are shown in Figure 10 (open circles) (also shown in Figure 5). We have also calculated the more traditional secular variation rates for the same time intervals. Figures 4 (a, b) illustrate how we calculate absolute PSV rate in 200-year increments. We have calculated the incremental absolute secular variation rates for the intervals 0-100 years and 100-200 years (labeled r1 and r2 in Figures 4 (a, b)) for each circularity interval and averaged them. The average absolute secular variation rates per 100 years averaged over a 200-year circularity interval are also plotted in Figure 10 (solid circles). It is clear that the narrow intervals of highest-rate circularity are also the intervals of highest-rate average absolute secular variation. Arrows in Figure 10 show 5 intervals of highest secular variation/circularity rate that seem to be common to most of the records. The high rate intervals tend to occur at the boundaries between clockwise and counter-clockwise circularity. This is clearest at the onset and termination of clockwise intervals B and F in Figure 10. Similar short intervals of high secular variation/circularity rate are noted in East Asia. But they do not generally occur at the same times as in Eastern North America.

Discussion

Geomagnetic secular variation has been associated with a variety of different fluid motions in the Outer Core. Some motions are 'linear' in the sense that they suggest consistent movement of dynamo sources in one direction through drift (westward, eastward, poleward). Another possibility is that localized fluid flow is analogous to a 'whirlpool' with magnetic directions 'spinning' clockwise or counterclockwise in response. Both of these types of motion should produce a series of open loops of the same type (either clockwise or counterclockwise) through time. However, our data suggest a 'teeter-totter' behavior with alternating clockwise and counter-clockwise motion. We never see two consecutive full clockwise or counterclockwise loops in either the Holocene Eastern North America PSV or the East Asia PSV (Lund, 2020).

It seems likely that a significant component of the Outer Core fluid flow (and resulting secular variation) oscillates back and forth between clockwise and clockwise states. Figure 5 suggests maybe 3 or 4 such oscillations within the last 3000 years in Eastern North America. This is seen in both estimates of circularity – circularity rates and larger –scale looping. This is also seen in Holocene East Asia (Lund, 2020). Previous PSV studies have sometimes estimated coherent intervals of circularity that last 6-10 thousand years (e.g., Lund and Banerjee, 1985). It may be that a more careful (regional) analysis, such as carried out here, might see evidence of more complexity in circularity than previously noted.

The amplitude and duration of coherent circularity in our study is distinctive. There are shorter intervals of clockwise or counterclockwise circularity, perhaps a little as 300-400 years in duration with relatively low circularity rates (or looping amplitudes). There is also evidence of at least one interval of circularity that lasts perhaps 1000-1200 years and has large amplitude looping. (Figure 7 top) Even larger clockwise loops (~1500 years) are seen in Holocene PSV from East Asia (Lund, 2020) (Figure 7 bottom).

The duration of coherent cyclicity also seems to be unbalanced. More than 2/3 of the last 3000 years in both Eastern North America and East Asia have been periods of clockwise circularity. Individual periods of counterclockwise circularity always last less than 1000 years and average ~700 years (Figure 7). Clockwise loops tend to average ~1000 years. It is not clear that there is such a bias between 3000-8000 ybp (Figure 9) but the data are less numerous or as high in quality as data for the last 3000 years (Figure 5).

Studies of anomalous historical secular variation intervals, which are termed geomagnetic jerks (Courtillot and LeMouel, 1976, 1984), have been associated with azimuthal (torsional) oscillations of outer core fluids on yearly intervals (Bloxham et al., 2002). Dumberry and Bloxham (2006) have also suggested that azimuthal oscillating flows might be a major cause of PSV on a millennial scale. If such zonal oscillations are combined regionally with more complex fluid flow that can lead to magnetic flux regeneration, then this might be the source of our circularity observations. Dumberry and Bloxham (2006) also suggested the azimuthal torsional oscillation might occur against a background of more steady fluid flow. This might account for the unbalanced time spent in clockwise versus counter-clockwise circularity. Torsional oscillation in the direction of steady flow might lead to longer time intervals of one sense of circularity (clockwise), while oscillations opposite the direction of steady flow might lead to shorter time intervals of the opposite sense of circularity (counter-clockwise).

Another distinctive feature that all the PSV records share is that circularity rates significantly increase for short periods of time (200-400 years) at the transitions from clockwise to counterclockwise looping (Figures 5, 10). To a lesser extent absolute secular variation rates are also highest at these times (Figure 10). These short intervals of high circularity rate (labeled B, D, and F in Figure 5 and 10) are quite distinctive with rates up to 5 times that of normal circularity intervals. Similar short interval increased rates of PSV have been noted in Holocene East Asia PSV

These short-duration intervals of accelerated secular variation with change in circularity direction seem to be broadly analogous to historic magnetic field jerks or impulses (Courtillot and LeMouel, 1976, 1984). These impulses are abrupt accelerations of normal historical secular variation that last only 1-2 years in the context of the last ~100-200 years of historical field variability. Gallet et al. (2003) studied archeomagnetic data from Europe and identified similar abrupt (10^2 years) cusps or hairpins in directional data that they associated with intervals of relatively high paleointensity. These short (~100-200 years) intervals of anomalously high PSV rate occur within the context of the last 2000-3000 years of PSV in Europe. Gallet et al. (2003) called these events archeomagnetic jerks and argued that they were intermediate between geomagnetic jerks (10^0 years) and magnetic field excursions (10^3 years). (It is probably better to refer to these a paleomagnetic jerks since they can be recorded in sediment PSV records as well as archeological time series.) It seems reasonable to argue that our short-duration intervals of accelerated secular variation with changes in circularity direction are also examples of paleomagnetic jerks or impulses. Altogether, these various 'short' intervals of anomalous secular variation rate that occur within the context of ongoing secular variation on a variety of time scales may reflect an intrinsic, chaotic element in the overall dynamo process.

Figure 11 shows the late Holocene central North American paleointensity record (Lund et al., 2021). This composite record included paleointensity estimates from the LEB, SEN, 2220, and ECS PSV records. Arrows indicate the highest rate circularity an overall PSV in our records (Figure 10). All of our accelerated intervals seem to be associated with relatively fast-changing intensity, either increasing or decreasing. There does not seem to be any indication of fast PSV at intensity highs or lows as was noted for East Asia (Lund, 2020). More regional studies are needed to carefully assess these relationships.

Conclusions

This study summarizes the pattern of directional paleomagnetic secular variation (PSV) in five previously published Holocene records from Eastern North America. Each record is high in resolution and well dated. We have developed equi-spaced (100-year increment) time series for the declinations and inclinations for the five sites and compared their overall directional variability. We see evidence of ten correlatable scalar features in both inclination and declination. These comparisons suggest that, to first order, these five PSV records all estimate the same regional pattern of PSV for Eastern North America.

We specifically focus on the clockwise or counter-clockwise motion of paleomagnetic directions (termed circularity) in these PSV records. We have used two techniques to estimate the directional circularity of each PSV record. We have first calculated the incremental rate and direction of motion (clockwise or counter-clockwise) in 200-year increments for each record over the last 3000-8000 years. We have separately used a more traditional technique of looking for discernable looping (full loops down to 1/2 loops) in individual records. We estimate the loop sizes, durations, and circularity direction.

We largely see the same pattern of circularity in both measurement techniques. There are seven intervals of oscillating circularity (clockwise versus counter-clockwise) in all five sites. They generally agree in timing and direction of circularity. We also see evidence for seven discernable directional loops alternating between clockwise and counter-clockwise in all five records. Both techniques suggest an oscillating, teeter-totter like, behavior to PSV circularity that must be due to the pattern of fluid flow/magnetic flux regeneration in the outer core. This teeter-totter behavior is unbalanced with more time spent in clockwise motion as in counter-clockwise motion. Less than 10% of the overall time series duration is spent in linear (not circulating) behavior. The loops tend to have a distribution of sizes and durations with smaller loops being shorter in duration (400-800 years) and bigger loops having longer durations (600-1200 years).

The teeter-totter alternation of clockwise versus counter-clockwise circularity is distinctive and may be a normal aspect of PSV. The alternation is not consistent with several traditional ideas about fluid flow (drift, whirling motion, simple convection). Recent studies have identified torsional oscillations as a source for both historical short-term (10^0) and millennial-scale (10^3) secular variation (Bloxham et al., 2002; Dumberry and Bloxham, 2006).

One particular feature of these circularity patterns bears special note. All five PSV records show short-tern (200-400 years) significant acceleration in circularity rate combined with change in circularity direction. We see evidence for five of these short intervals. These features are also intervals of the fastest regular secular variation rates in all the records. These features are analogous to geomagnetic jerks (Courtillot and LeMouel, 1976, 1984) in that they are short intervals of anomalous acceleration. But geomagnetic jerks occur historically every 20-40 years and last only 1-2 years. Gallet et al. (2003) showed evidence in PSV for similar anomalous acceleration intervals (~10^2 yrs), which they termed archeomagnetic jerks. We think our anomalous intervals are comparable to those of Gallet et al. (2003). We think these features are a natural and common aspect of directional PSV, but more regional PSV studies are needed to test that possibility.

References

Alldredge, l., and L. Hurwitz, 1964, Radial dipoles as sources of the Earth's magnetic field, J. Geopjys. Res., 69, 2631-2640.

Barletta, F., G. St.Onge, J. Stoner, P.Lajeunesse, and J Locat, 2010, A high-resolution Holocene paleomagnetic secular variation and relative paleointensity stack from eastern Canada, Earth Planet. Sci. Lett., 298, 162-174.

Bauer, L., 1895, On the distribution and the secular variation of terrestrial magnetism, Amer. J. Sci., 50, 314-325.

Bloxham, J., D. Gubbins, and A. Jackson, Geomagnetic secular variation, Phil. Trans. Roy. Soc. London A, v. 329, p. 415-502, 1989.

Bloxham, Jeremy; Zatman, Stephen; Dumberry, Mathieu (November 2002). "The origin of geomagnetic jerks". Nature. 420 (6911): 65–68. doi:10.1038/nature01134

Constable, C., C. Johnson, and S. Lund, 2000, Global geomagnetic field models for the past 3000 years: transient or permanent flux lobes?, Phil. Trans., R. Soc. London, 358, 99-108.

Constable, C., 2011, Modeling the geomagnetic field from synthesis of paleomagnetic data, Phys. Earth Planet. Int., 187, 109-117.

Courtillot, V., and J. Le Mouel, 1976, On the long-period variations of the Earth's magnetic field from 2 months to 20 years., J. Geophys. Res., 81, 2941-2950.

Courtillot, V., and J. Le Mouel, 1984, Geomagnetic secular variation impulses, Nature, 311, 709-716.

Davies, C. and C. Constable, 2018, Searching for geomagnetic spikes in numerical dynamo simulations, Earth. Planet. Sci. Lett., 504, 72-83.

Dodson, R., 1979, Counterclockwise precession of the geomagnetic field vector and westward drift of the non-dipole field, J. Geophys. Res., 84, 637-644.

Doell, R. , and A. Cox, 1965, Paleomagnetism of Hawaii lava flows,J. Geophys. Res., 70, 3377-3405.

Dumberry, M., and J. Bloxham, 2006, Azimuthal flows in the Earth's core and changes in length of data at millennial timescales, Geophys. J. Int., 165, 32-46.

Evans, M. E., Paleomagnetic evidence for stationary sources of geomagnetic secular variation, Phys. Earth Planet. Int., v. 35, p. 223-226, 1984.

Gallet, Y., A. Genevy, and V. Courtillot, 2003, On the possible occurrence of 'archeomagnetic jerks' in the geomagnetic field over the last three millennia, Earth Planet. Sci. Lett., 214, 237-242.

Gubbins, D., and J. Bloxham, Morphology of the geomagnetic field and implications for the geodynamo, Nature, v. 325, p. 509-511, 1987.

Hagee, V. L., and P. Olson, 1989, An analysis of paleomagnetic secular variation in the Holocene, Phys. Earth Planet. Int., V. 56, p.266-284.

Itota, C., M. Hyodo, and K. Yaskawa, 1997, Long-term features of drifting and standing non-dipole fields as determined from Holocene paleomagnetic secular variation, Geophys. J. Int., 130, 390-404.

Jackson, A., A. Jonkers, and M. Walker, 2000, Four centuries of geomagnetic secular variation from historical records, Phil. Trans. Roy. Soc. A, 358, 957-990.

Kawai, N., K. Hirooka, and S. Sasajima, Counterclockwise rotation of the geomagnetic dipole axis revealed in the world-wide archeo-secular variations, Proc. Japan Acad., v. 41, p. 398-403, 1965.

King, J., 1983. Geomagnetic secular variation curves for the northeastern North America for the last 9000 years, unpublished Ph.D. dissertatiom, Uni. Minnesota.

King, J., S. Banerjee, J. Marvin, and S. Lund, 1983, Use of small-amplitude paleomagnetic fluctuations for correlations and dating of continental climatic changes, Paleogeog., Paleoclim., Paleoecol., 42, 167-283.

Korte, M., C. Constable, F. Donadini, and R. Holmes, 2011, Reconstructing the Holocene geomagnetic field, Earth Planet. Sci. Lett., 312, 497-505.

Lund, S., 1996, A comparison of Holocene paleomagnetic secular variation records from North America, J. Geophys. Res., v. 101, p. 8007-8024.

Lund, S., 2020, Regional character of geomagnetic field directional circularity: Holocene East Asia, Phys. Earth. Planet. Int., 308, 106572.

Lund, S. and S. K. Banerjee, 1985, Late Quarternary paleomagnetic field secular variation from two Minnesota lakes, J. Geophys. Res., V. 90, p. 803-825.

Lund, S., J. C. Liddicoat, K. L. Lajoie, T. L. Henyey and Steve W. Robinson, 1988, Paleomagnetic evidence for long-term (10^4 year) memory and periodic behavior in the Earth's core dynamo process. Geophysical Research Letters , V. 15, p. 1101-1104.

Lund, S., L. Keigwin, and D. Darby, 2016, Character of paleomagnetic secular variation in the tangent cylinder: evidence from the Chukchi Sea, Phys. Earth Planet. Int., 256, 49-58.

Lund, S., M. Richardson, K. Verosub, J. King, D. Champion, and G. St.Onge, 2021, Comparison and renormalization of Holocene paleointensity records from central North America, Earth and Space Sci., 8, e2021EAOO1900, https://doi.org/10.1029/2021EADOO 1900.

Merrill, R., M. McElhinny, and P. McFadden, 1998, The magnetic field of the Earth, Academic Press, 533 pp.

Negrini, R., DB Erbes, AP Roberts, KL Verosub, AM Sarna-Wojcicki, 1994, Journal of Geophysical Research: Solid Earth 99 (B12), 24105-24119.

Olson, P., and L. Hagee, 1987, Dynamo waves and paleomagnetic secular variation, Geophys. Astron. Soc., 88, 139-159.

Runcorn, S., 1959, On the theory of the geomagnetic secular variation, Ann. De Geophys., 15, 87-92.

Smith, G., and K.M. Creer, 1986, Analysis of geomagnetic secular variations 10000 to 30000 yrs BP, Lac du Bouchet, FrancePhys. Earth Planet. Inter., 44 (1986), pp. 1-14

Skiles, D., 1970, A method of inferring the direction of drift of the geomagnetic field from paleomagnetic data, J. Geomag. Geoelect., 22, 441-462.

St. Onge, G., J. Stoner, and C. Hillaire-Marcel, 2003. Holocene paleomagnetic records from the St. Lawrence Estuary, eastern Canada,: centennial to millennial scale geomagnetic modulation of cosmogenic isotopes, Earth Planet. Sci. Lett., 209, 113-130.

Thompson, R. and D. R. Barraclough, Geomagnetic secular variation based on Spherical Harmonic and Cross Validation analyses of historical and archaeomagnetic data, J. Geomag. Geoelectr., 34, 245-263, 1982.

Turner, G. , M. Evens, and I. Hussin, 1982, A geomagnetic secular variation study (31000-19500 bp) in western Canada, Geophys. J. R. Astron. Soc., 71, 159-171.

Figure Captions:

Figure 1: Map of Eastern North America showing the sites of eight paleomagnetic studies discussed in the text.

Figure 2: A summary of the best quality PSV inclination records for Eastern North America over the last 3000 years. Smallsolid circles are PSV data from published records; lines to either side indicate ± 1-sigma. Large solid circles are equi-spaced model inclination time series for each record (100 year spacing). Open squares indicate estimates of historical field for each locality determined by Jackson et al. (2000). The typical difference between model and original data is less than ±1°.

Figure 3: A summary of the best quality PSV declination records for Eastern North America over the last 3000 years. Small closed circles are PSV data from published records; lines to either side indicate ± 1-sigma. Larger solid circles are equi-spaced model declination time series for each record (100 year spacing). Open squares indicate estimates of historical field for each locality determined by Jackson et al. (2000). The typical difference between model and original data is less than ±1°.

Figure 4: Graphical representation of the methodology used to calculate true circularity rates (a, b) and looping patterns (c). Areas of looping in a and b are measured in arc degrees squared (area).

Figure 5: The results of two methods for calculating circularity for each model time series. True circularity rates are plotted for 3-point (open circles) and 5-point (solid circles) circularity at each site in units of arc degrees squared (area) At left in each column is an alphanumeric zonation of intervals dominated by clockwise (grey intervals) and counterclockwise (white intervals) circularity. At right, are columns labeled with greek lettering that indicate intervals of distinctive looping (black columns have clockwise looping and white columns have counterclockwise looping).

Figure 6: Bauer plots of inclination versus declination movement versus time within each time series. Clockwise (C) or counter-clockwise (CC) loops are shown for clarity.

Figure 7: Plot of individual discernable loops by duration versus overall amplitude. Figure 7 top is data from Eastern North America. Figure 7 bottom is data

from East Asia. Amplitudes are calculated in Table 2. The straight-line fit through the data give a sense to shorter (longer) duration loops being smaller (larger) in amplitude.

Figure 8: PSVMOD2.0 inclination and declination models of the three longest PSV records from the Eastern North America region.

Figure 9: Circularity calculation for the three longest PSV records. True circularity rates are plotted for 3-point (open circles) and 5-point (solid circles) circularity at each site. The alphanumeric letters correspond to the same zones plotted in Figure 5.

Figure 10: Comparison of true circularity rate (arc degree squared, 3-pt average, open circles) with absolute interval secular variation rate (arc degrees over same interval as circularity) irrespective of directional circularity.

Figure 11: Paleointensity record for central North America. Arrows indicate intervals of fast circularity or PSV rate.

Figures 1-11.

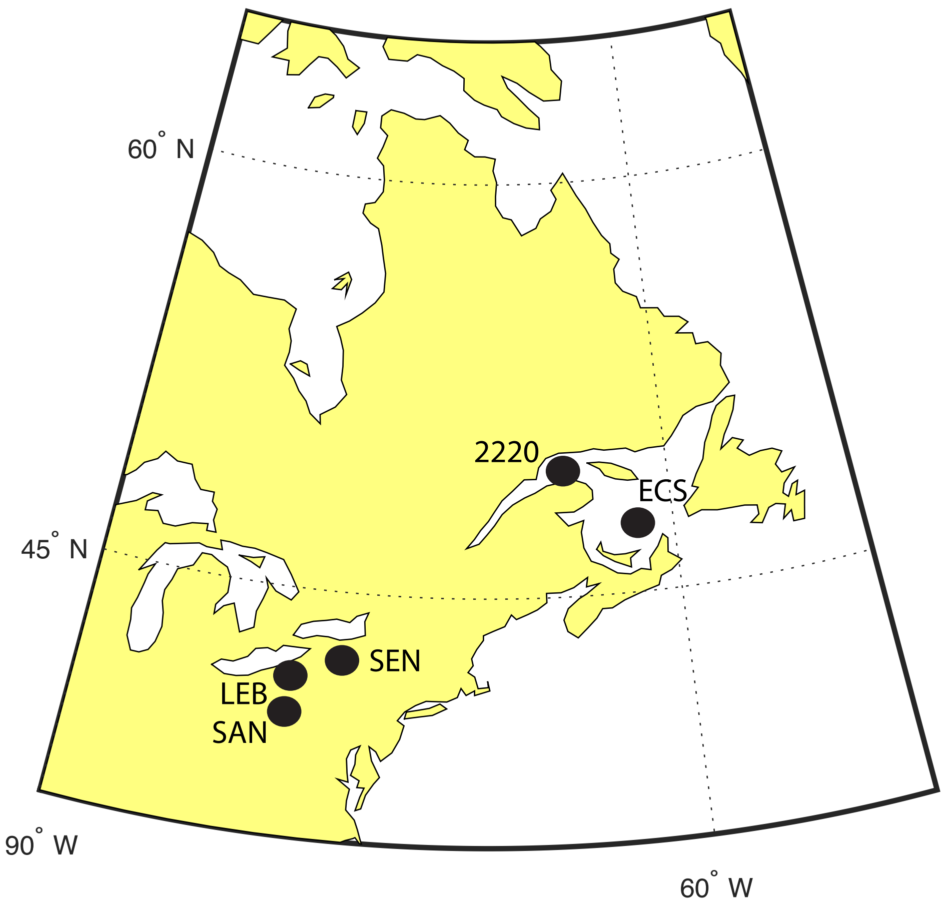

Figure 1

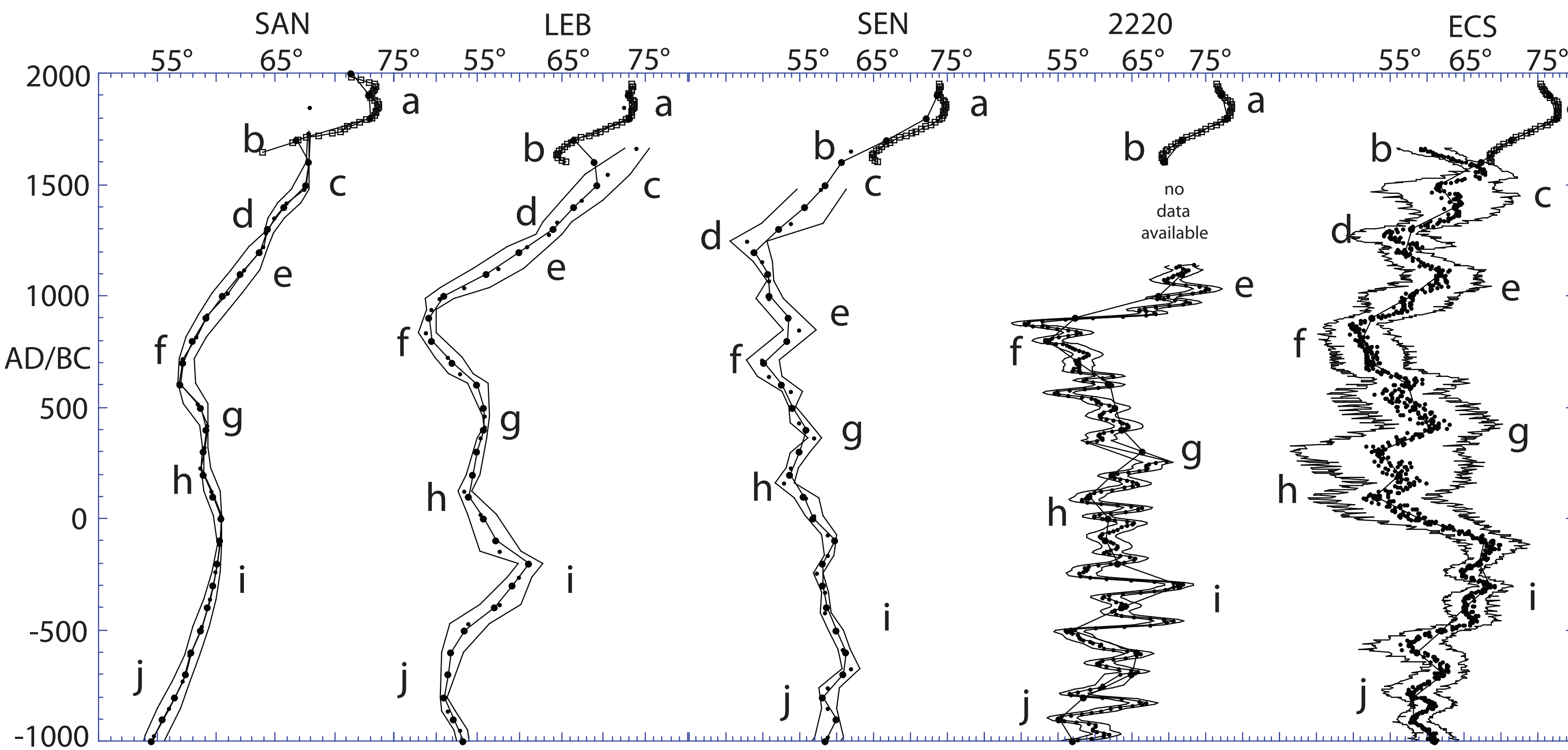
SAN
LEB
SEN
2220
ECS
55°
65°
75°
2000
1500
1000
AD/BC
500
0
-500
-1000
a
b
c
d
e
f
g
h
i
j
no
data
available

Figure 2

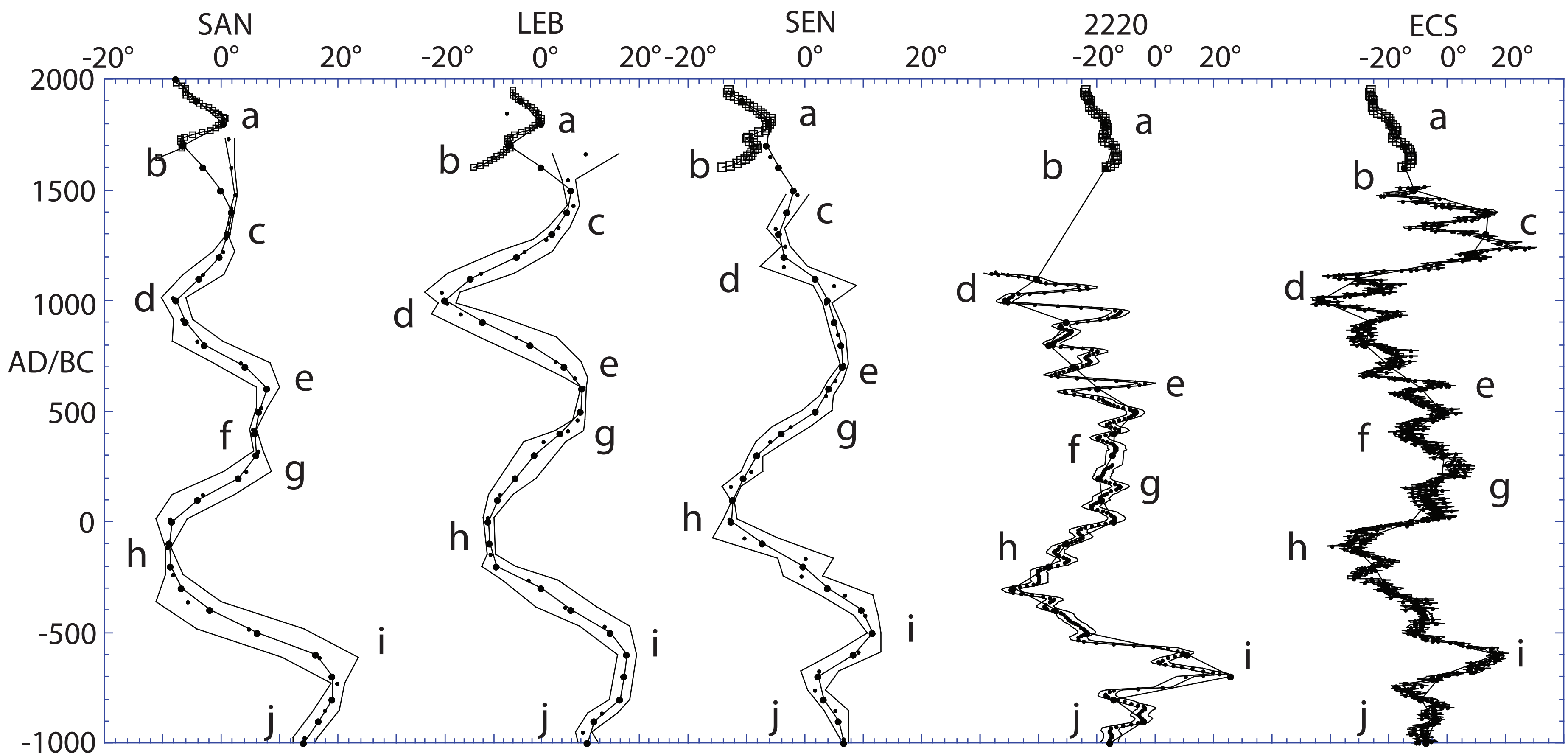
SAN
LEB
SEN
2220
ECS
-20°
0°
20°
2000
1500
1000
AD/BC
500
0
-500
-1000
a
b
c
d
e
f
g
h
i
j

Figure 3

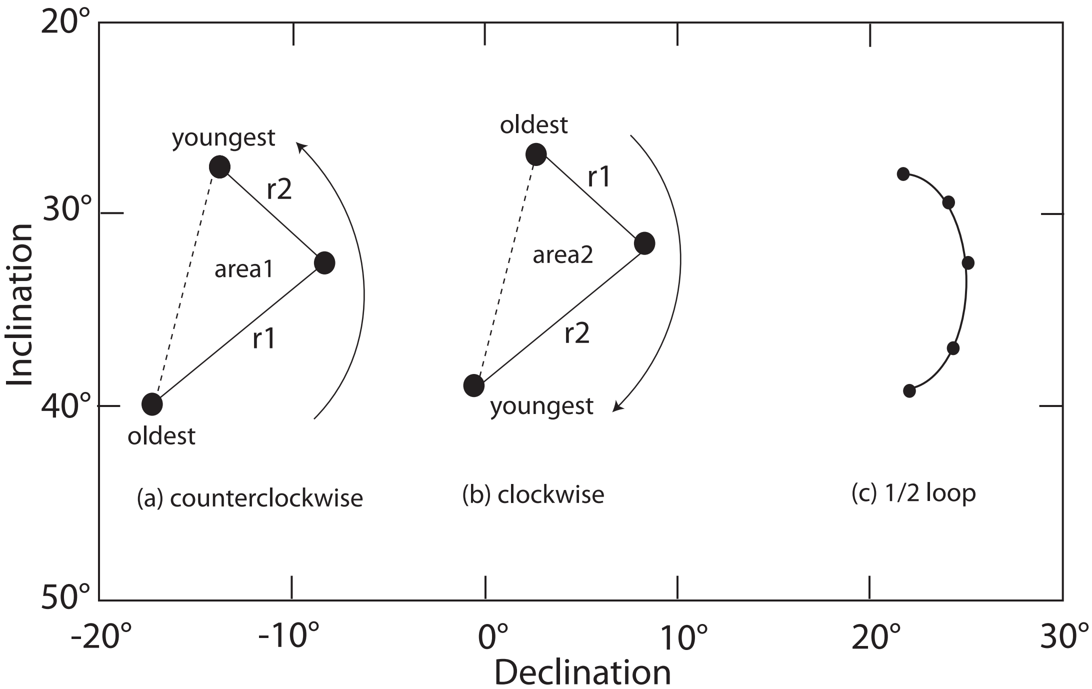
20°
30°
40°
50°
Inclination
youngest
r2
area1
r1
oldest
oldest
r1
area2
r2
youngest
(a) counterclockwise
(b) clockwise
(c) 1/2 loop
-20°
-10°
0°
10°
20°
30°
Declination

Figure 4

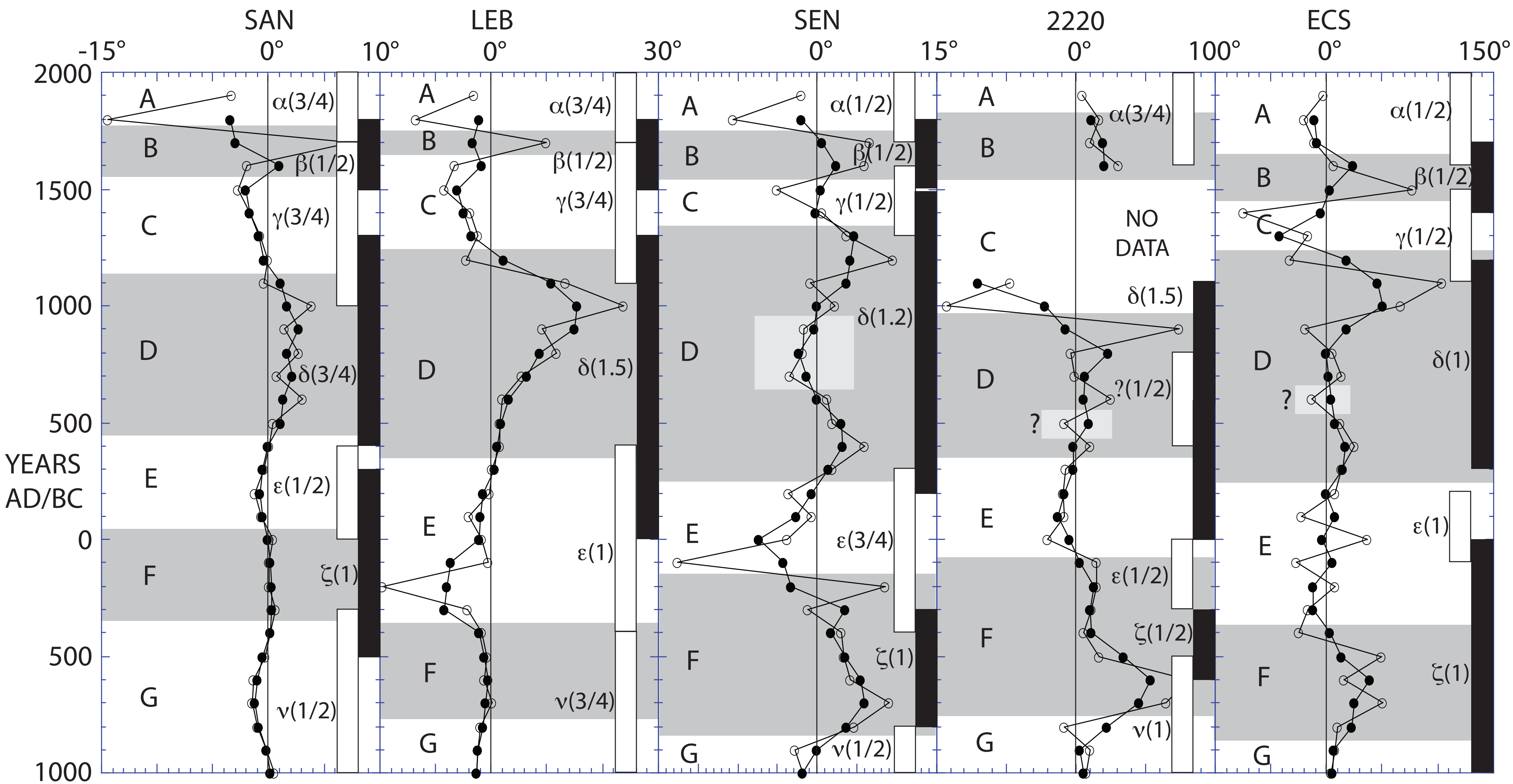
SAN
LEB
SEN
2220
ECS
-15°
0°
10°
30°
15°
100°
150°
2000
1500
1000
500
YEARS
AD/BC
0
500
1000
A
B
C
D
E
F
G
α(3/4)
β(1/2)
γ(3/4)
δ(3/4)
ε(1/2)
ζ(1)
ν(1/2)
δ(1.5)
ε(1)
ν(3/4)
α(1/2)
γ(1/2)
δ(1.2)
ε(3/4)
NO
DATA
?(1/2)
?
ε(1/2)
ζ(1/2)
ν(1)
δ(1)

Figure 5

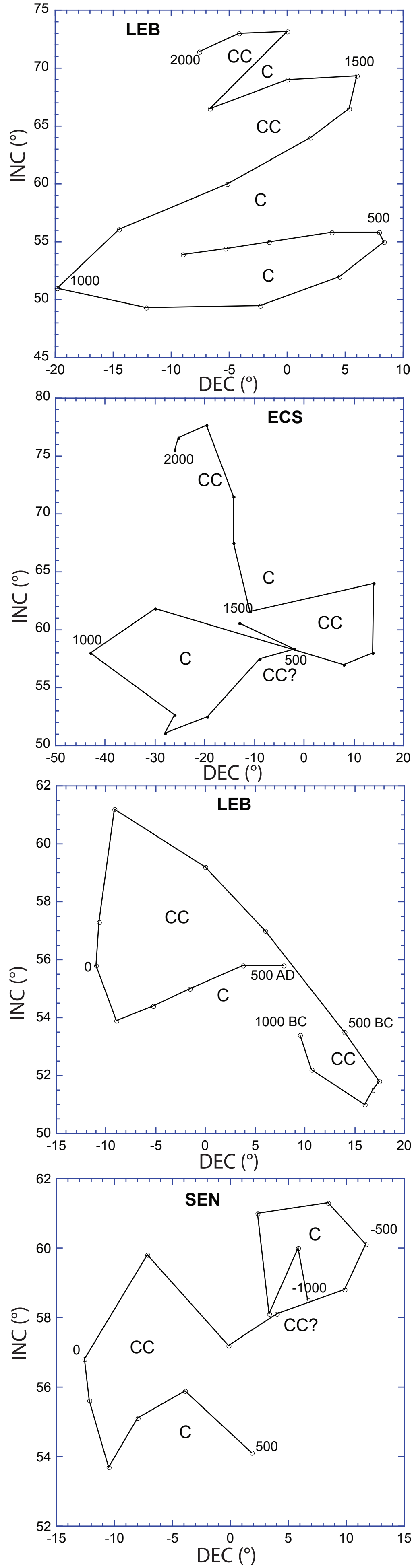
LEB
2000
CC
C
1500
CC
C
500
1000
C
INC (°)
DEC (°)
ECS
2000
CC
C
1500
CC
1000
C
500
CC?
LEB
CC
0
500 AD
C
1000 BC
500 BC
CC
SEN
C
-500
-1000
CC?
0
CC
C
500

Figure 6

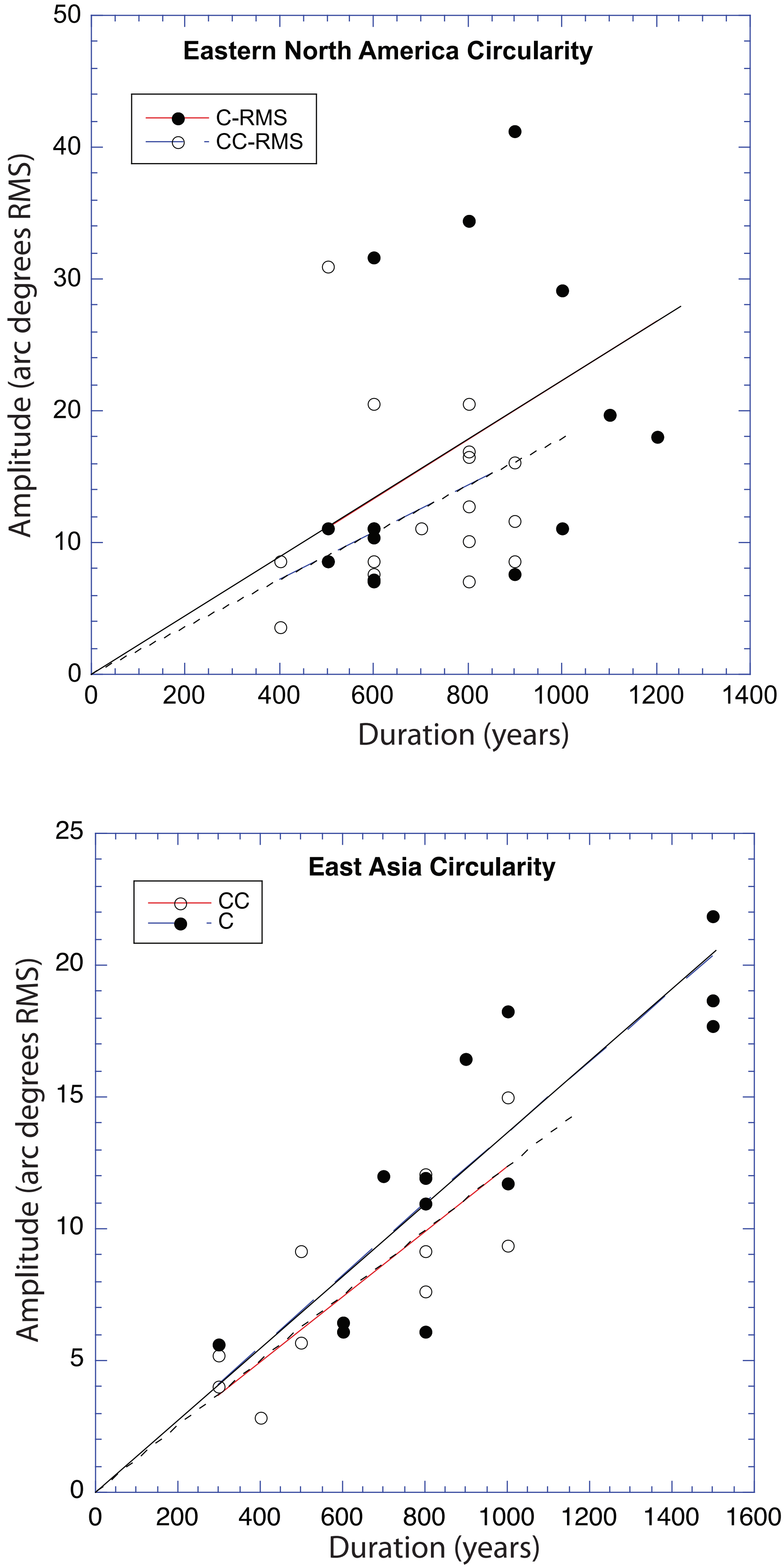
Eastern North America Circularity
C-RMS
CC-RMS
Amplitude (arc degrees RMS)
Duration (years)
0
10
20
30
40
50
0
200
400
600
800
1000
1200
1400
East Asia Circularity
CC
C
Amplitude (arc degrees RMS)
Duration (years)
0
5
10
15
20
25
0
200
400
600
800
1000
1200
1400
1600

Figure 7

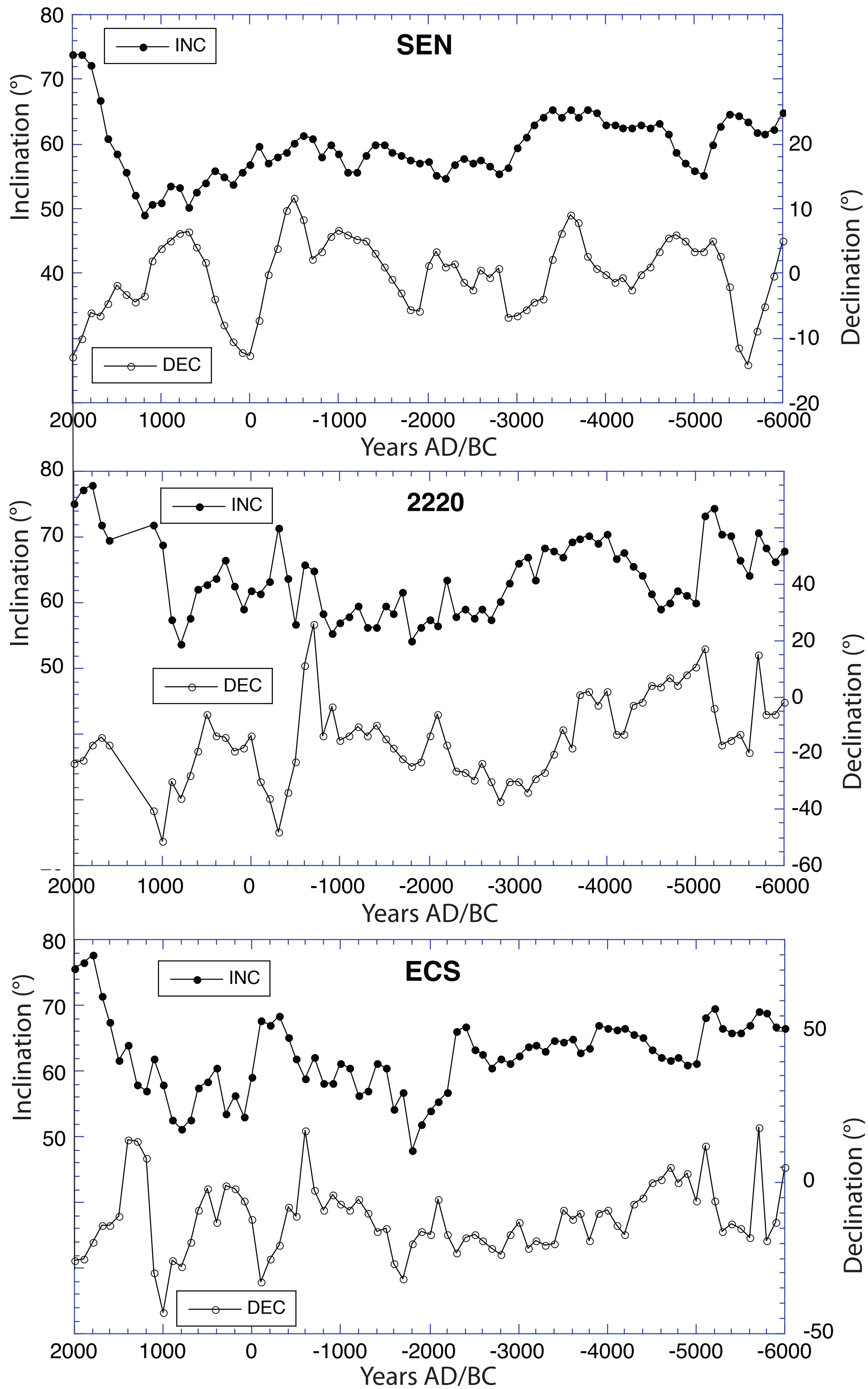
SEN
INC
DEC
Inclination (°)
Declination (°)
Years AD/BC
2220
INC
DEC
Inclination (°)
Declination (°)
Years AD/BC
ECS
INC
DEC
Inclination (°)
Declination (°)
Years AD/BC

Figure 8

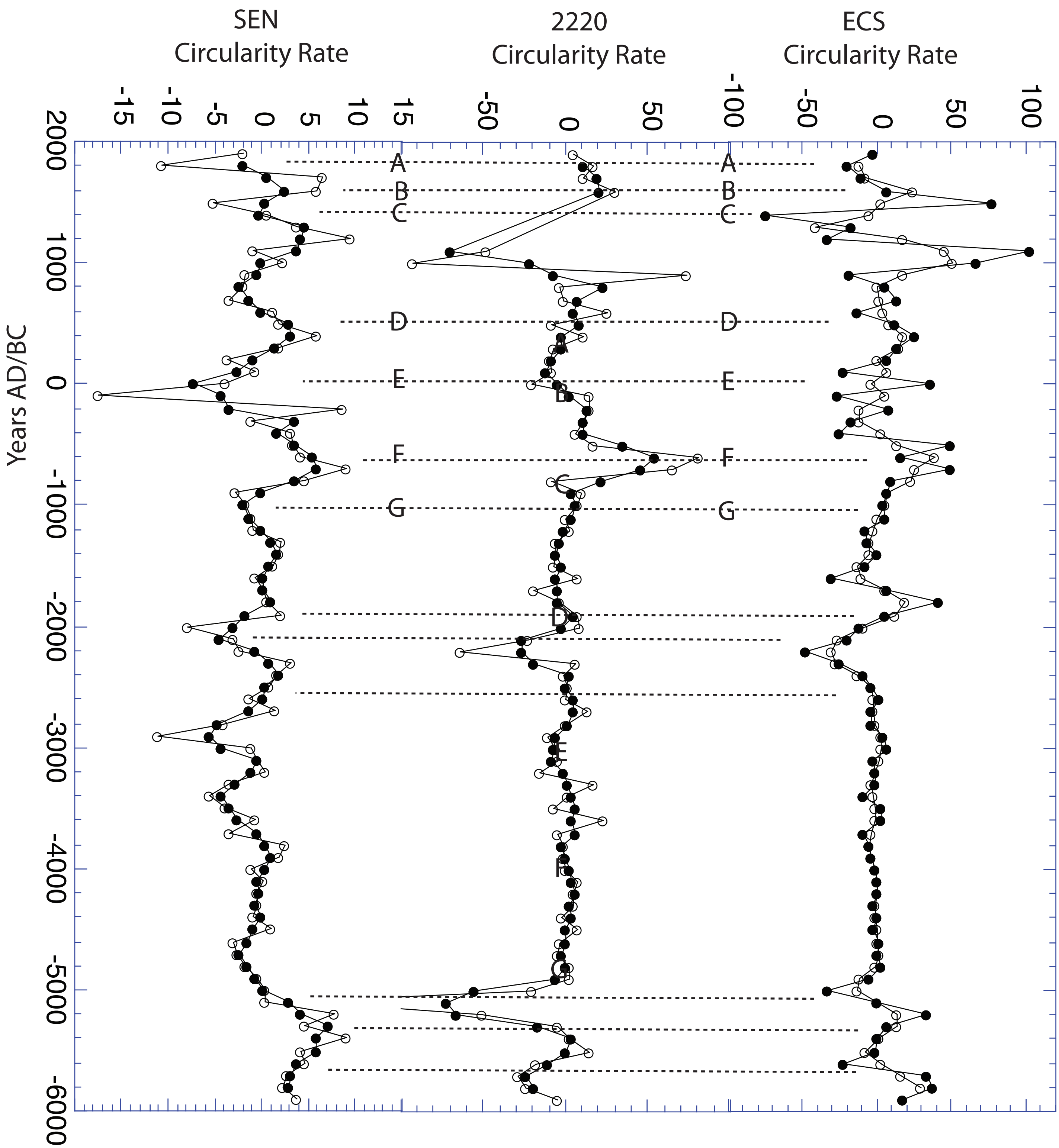
ECS
Circularity Rate
2220
Circularity Rate
SEN
Circularity Rate
Years AD/BC
A
B
C
D
E
F
G

Figure 9

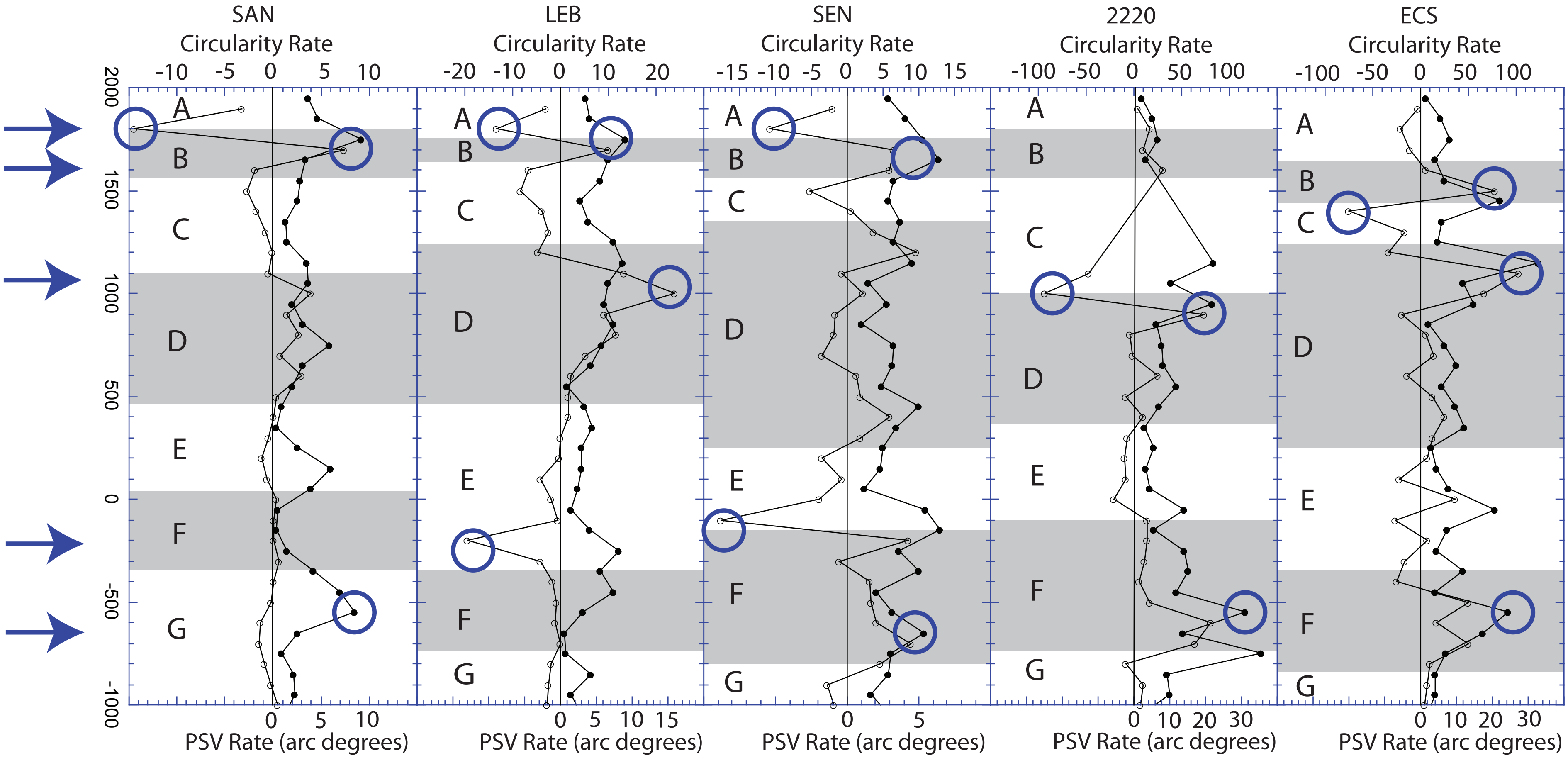
SAN
Circularity Rate
LEB
Circularity Rate
SEN
Circularity Rate
2220
Circularity Rate
ECS
Circularity Rate
A
B
C
D
E
F
G
PSV Rate (arc degrees)
PSV Rate (arc degrees)
PSV Rate (arc degrees)
PSV Rate (arc degrees)
PSV Rate (arc degrees)

Figure 10

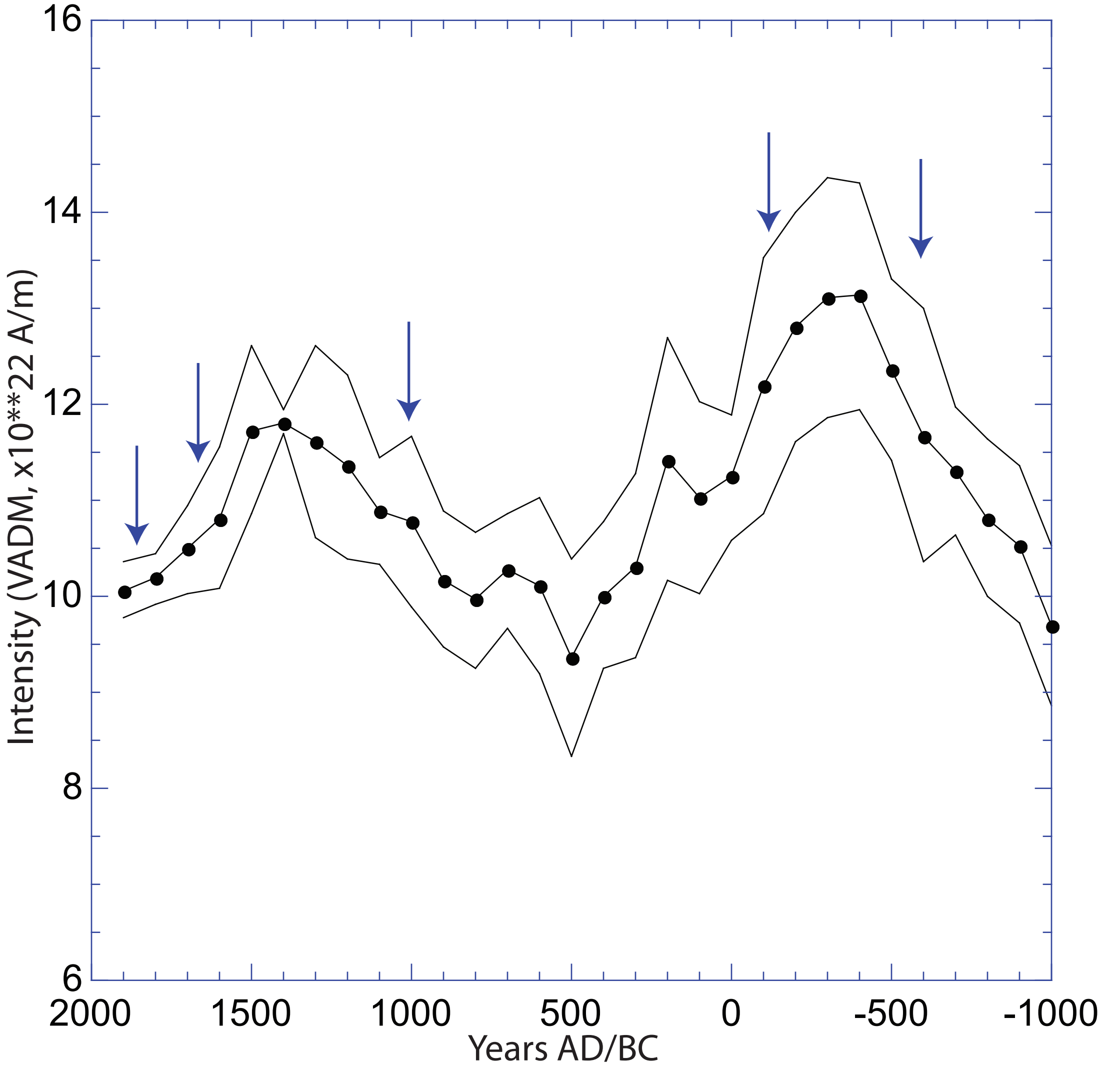
16
14
12
10
8
6
Intensity (VADM, x10**22 A/m)
2000
1500
1000
500
0
-500
-1000
Years AD/BC

APPENDIX 1: PSVMOD2.0 datasets for Sandy Lake (SAN), Lake Lebeouf (LEB), Sene

AD/BC	SAN-INC	SAN-DEC		LEB-INC	LEB-DEC
2000	71.4	-7.6			
1900	72.9	-4.2		73	-4.2
1800	73.1	0.6		73.2	0
1700	66.8	-6.5		66.5	-6.7
1600	67.8	-3		69	0
1500	67.6	0		69.3	6
1400	65.7	1.8		66.5	5.3
1300	64.4	1.3		64	2
1200	63.7	-0.2		60	-5.2
1100	62.1	-3.8		56.1	-14.5
1000	60.6	-7.7		51	-19.8
900	59.2	-6.1		49.3	-12.2
800	58	-2.7		49.5	-2.3
700	57.2	4.2		52	4.5
600	57	7.9		55	8.3
500	58.7	6.6		55.8	7.9
400	59.2	5.8		55.8	3.8
300	58.9	6		55	-1.6
200	58.9	3		54.4	-5.3
100	59.7	-3.9		53.9	-9
0	60.4	-8.4		55.8	-11
-100	60.3	-8.9		57.3	-10.7
-200	60.1	-8.5		61.2	-9.2
-300	59.7	-6.8		59.2	0
-400	59.3	-1.9		57	6
-500	58.7	6.2		53.5	14
-600	57.9	16.2		51.8	17.5
-700	57.4	19.2		51.5	16.8
-800	56.5	19		51	16
-900	55.5	16.7		52.2	10.7
-1000	54.5	14.1		53.4	9.5
-1100	53.7	13		54	13.3
-1200	53	12.7		52.8	14
-1300	53.1	10.3		52.2	12.7
-1400	54	7.5		51.8	6.5
-1500	55.2	4.5		53	-2.7
-1600	56	3		54.7	-7.8

-1700	57.4	1.5		56	-8.5
-1800	58.5	-0.1		58.3	-2
-1900	59.1	-1.6		59.5	0.8
-2000	59.1	-2.2			
-2100	59.3	-2			
-2200	59.9	-0.3			
-2300	60.9	1.5			
-2400	61.5	0.7			
-2500	62.1	1			
-2600	62.6	1.3			
-2700	63.4	0.5			
-2800	64.3	-0.4			
-2900	65	-1.6			
-3000	65.9	-2.3			
-3100	67	-3			
-3200	67.7	-2.3			
-3300	67.9	-1.9			
-3400	66.6	0.3			
-3500	64.2	3.4			
-3600	62.5	6			
-3700	62.2	4.9			
-3800	62.4	0.3			
-3900	62.7	-3.6			
-4000					
-4100					
-4200					
-4300					
-4400					
-4500					
-4600					
-4700					
-4800					
-4900					
-5000					
-5100					
-5200					
-5300					
-5400					
-5500					
-5600					
-5700					

-5800
-5900
-6000

ca Lae (SEN), core 2220 (2220) and the East Canada Stack (ECS).

SEN-INC	SEN-DEC	2220-INC	2220-DEC	ECS-INC
73.8	-7	77.2	-22.3	76.6
72.2	-6.1	78	-17	77.7
66.9	-6.5	71.9	-14.4	71.5
60.8	-4.5	69.5	-16.8	67.5
58.5	-1.8			61.6
55.8	-3.1			64
52.2	-4.4			58
49.001	-3.5			57
50.7	2	71.8	-40.2	61.8
51	3.9	68.8	-51	58
53.6	5.1	57.5	-30	52.7
53.4	6.3	53.7	-36	51.1
50.2	6.6	57.8	-27.7	52.5
52.7	4.2	62.1	-19.5	57.5
54.1	1.8	62.8	-6.3	58.3
55.9	-3.9	63.7	-14	60.6
55.1	-8	66.5	-14.5	53.5
53.7	-10.5	62.5	-19	56.3
55.6	-12.2	59.2	-18.2	53
56.8	-12.6	61.8	-14	59
59.8	-7.2	61.5	-30	67.8
58.2	-0.2	63.2	-36	67
58.1	4	71.5	-48.2	68.5
58.8	9.8	63.7	-34	65.2
60.1	11.7	56.8	-23	62
61.3	8.4	65.8	11	58.8
61	2.3	65	26	62.2
58.1	3.3	58.5	-14	58.2
60	5.8	55.3	-3.5	58.2
58.5	6.7	57	-15.5	61.2
55.6	6	58	-13.8	60.5
55.6	5.3	59.5	-10.3	56.2
58.2	5	56.3	-14	57
59.9	3.2	56.3	-10.2	61.3
59.9	1	59.5	-15	60.4
58.8	-0.9	58.5	-18	54.3

58.4	-2.9	61.7	-22	56.8
57.6	-5.6	54.3	-24.5	48
57	-5.9	56.2	-23	52
57.3	1.2	57.4	-14	54
55.2	3.5	56.5	-6	55.4
54.8	1	63.5	-17	56.8
56.8	1.6	58	-26.5	66
57.9	-1.3	59	-27	66.7
57.2	-2.5	57.8	-29.5	63.2
57.7	0.5	59	-23.8	62.5
56.7	-0.5	57.5	-30	60.6
55.4	0.9	60.3	-37	61.8
56.5	-6.7	63	-30	61.3
59.4	-6.5	66	-30	62.3
61.2	-5.6	67	-34	63.8
63	-4.3	63.6	-29	64
64.2	-3.9	68.5	-27	63.1
65.3	2.3	68	-20.3	64.7
64.2	6.3	67	-11.5	64.5
65.3	9.2	69.3	-18	65
64.3	7.8	69.7	1	62.9
65.5	2.8	70.2	2	63.5
65	0.7	69.2	-3	66.9
63	-0.2	70.4	2	66.5
63	-1.3	66.7	-13.5	66.4
62.5	-0.5	67.7	-13	66.5
62.5	-2.6	65.5	-3	65.7
63	-0.2	64.2	-2	65.1
62.5	1	61.5	4	63.4
63.3	3.3	59	3.8	62.2
61.5	5.5	60	7	61.7
58.8	6	61.8	4	62.2
57.2	5	61.3	8	60.9
55.9	3.5	60	10.5	61.1
55.2	3.4	73.3	17	68.1
59.9	5.1	74.5	-4.3	69.5
62.7	2.8	70.5	-17	66.5
64.6	-2.1	70.3	-15.5	65.9
64.5	-11.5	66.5	-13.5	65.9
63.6	-14	64.3	-20	67
61.8	-8.8	70.7	15	69

61.5	-5	68.5	-6	68.8
62.3	-0.3	66.2	-6	66.8
64.8	5	68	-2	66.6

ECS-DEC	T
-25.2	
-19.6	
-14.2	
-14.2	
-11	
14	
13.7	
8	
-30	
-43	
-26	
-28	
-19.5	
-9	
-2	
-13	
-1	
-2	
-6	
-12	
-33	
-25	
-20.5	
-8	
-11	
17	
-2.5	
-9	
-4	
-7	
-9	
-5.8	
-10	
-16	
-15	
-27	

-32
-20
-16
-17
-5.8
-17
-23
-18
-17
-19
-21.5
-23.5
-17
-13
-21.5
-19
-20.5
-20
-9
-12
-10
-19
-10
-9
-14
-17
-7
-5
0
1
5
0
3
-6
12
-6
-16
-13.8
-15
-18
18

-19
-13
5

Table 1: Summary of Eastern North American Paleomagnetic Secular Variation Records Used in This Study

Site Code	Site Location	Lat. (°N)	Lon. (°E)	Age Range (YBP)	Date Type	Final Sed. Rate	Qual.
2220	St. Lawr.	48.6	291.4	0-8000	C14	~100 cm/ky	A
ECS	St. Lawr.	48.2	295.5	0-8000	>10 C14	~100 cm/ky	A
LEB	Lake LeBeouf	41.9	280.1	0-4000	6 derived	~200 cm/ky	A
SAN	Sandy Lake	41.3	279.9	0-6000	8 C14	~180 cm/ky	A
SEN	Seneca Lake	43.0	286	0-8000	13 C14	~150 cm/ky	A

Table 2: summary of circularity timing and direction for the last 3000 years.

SITE	FEATURE	INT.	Circ.	LOOP PART	INC	DEC	RMS	DURATION	C-RMS	CC-RMS
SAN										
	α	2000-1700	CC	0.75	5	7	8.6	500		8.6
	β	1800-1500	C	0.5	4	6	7.2	600	7.2	
	γ	1700-1000	CC	0.75	6	10	11.7	900		11.7
	δ	1300-400	C	0.75	10	15	18.0	1200	18.0	
	ε	400-0	CC	0.5	2	10	10.2	800		10.2
	ζ	400-500BC	C	1.0	3	7	7.6	900	7.6	
	ν	300BC-1000BC	CC	0.5	5	10	11.2	700		11.2
LEB										
	α	2000-1700	CC	0.75	5	7	8.6	400		8.6
	β	1800-1500	C	0.5	5	5	7.07	600	7.1	
	γ	1700-1100	CC	0.75	8	10	12.8	800		12.8
	δ	1300-0	C	1.5	15	25	29.2	100	29.2	
	ε	400-400BC	CC	1.0	7	15	16.5	800		16.5
	ζ	-	-							
	ν	300BC-1000BC	CC	0.75	5	7	8.6	900		8.6
SEN										
	α	2000-1700	CC	0.5	5	7	8.6	600		8.6
	β	1800-1500	C	0.5	10	3	10.4	600	10.4	
	γ	1600-1300	CC	0.5	7	3	7.6	600		7.6
	δ	1500-200	C	1.25	10	17	19.7	1100	19.7	
	ε	300-400BC	CC	0.75	6	15	16.2	900		16.2
	ζ	300BC-800BC	C	1.0	5	7	8.6	500	8.6	
	ν	800BC-1000BC	CC	0.5	2	3	3.6	400		3.6
2220										
	α	2000-1600	CC	0.75	5	10	11.2	600		11.2
	β	1100-600	C	0.75	17	30	34.5	800	34.5	
	γ	800-400	CC	0.5	5	20	20.6	800		20.6
	δ	600-0	C	0.5	5	10	11.2	1000	11.2	
	ε	0-300BC	CC	0.5	5	10	11.2	600		11.2
	ζ	300BC-600BC	C	0.5	10	30	31.6	600	31.6	
	ν	500BC-1000BC	CC	1.0	10	30	31.0	500		31.0
ECS										
	α	2000-1600	CC	0.5	5	5	7.1	800		7.1
	β	1700-1400	C	0.5	10	5	11.2	600	11.2	
	γ	1500-1100	CC	0.75	5	20	20.6	600		20.6
	δ	1200-300	C	1.0	10	40	41.2	900	41.2	
	ε	200-600BC	CC	1.0	8	15	17.0	800		17.0
	ζ	500BC-1000BC	C	1.0	5	10	11.2	500	11.2	
	ν	-	-							